Koufos, K., & Dettmann, C. P. (Accepted/In press). The Meta Distribution of the SIR in Linear Motorway VANETs. *IEEE Transactions on Communications*, *67*(12), 8696-8706. [8830403]. https://doi.org/10.1109/TCOMM.2019.2940659

The Meta Distribution of the SIR in Linear Motorway VANETs

Konstantinos Koufos and Carl P. Dettmann

***Abstract*—The meta distribution of the signal-to-interference-ratio (SIR) is an important performance indicator for wireless networks because, for ergodic point processes, it describes the fraction of scheduled links that achieve certain reliability, conditionally on the point process. In this paper, we calculate the moments of the meta distribution in vehicular ad hoc networks (VANETs) along high-speed motorways. Due to the high speeds, the drivers maintain large safety distances, and the Poisson point process (PPP) becomes a poor deployment model. Because of that, we model the distribution of inter-vehicle distance equal to the sum of a constant hardcore distance and an exponentially distributed random variable. We design a novel *discretization model* for the locations of vehicles which can be used to approximate well the meta distribution of the SIR due to the hardcore process. We validate the model against synthetic motorway traces. On the other hand, the PPP overestimates significantly the coefficient-of-variation of the meta distribution due to the hardcore process, and its predictions fail. In addition, we show that the calculation of the meta distribution becomes especially meaningful in the upper tail of the SIR distribution.**

***Index Terms*—Headway distance models, probability generating functional, reduced Palm measure, synthetic mobility traces.**

I. Introduction

The long-term vision of having vehicles communicating with each other for improving traffic flow, enabling automated driving, etc. is not far from reality [1]. The first standardization actions started in 1999, once the Federal Communication Commission in U.S. allocated 75 MHz of spectrum in the 5.9 GHz band for dedicated short-range communication [2]. In 2008, the European Commission set aside 30 MHz for cooperative intelligent transport systems. Since 2010, the technology amendment IEEE 802.11p has been the basis for worldwide PHY/MAC layer standards supporting Vehicle-to-Vehicle (V2V) communication in the 5.9 GHz band. In addition, the V2V communication will be secured under the umbrella of cellular LTE networks [3].

The performance of Vehicular ad hoc networks (VANETs) has been extensively studied during the past three decades using measurements and simulations, see for instance [4], [5] and the references therein. Unfortunately, both methods lack scalability. Recently, analytical tools, like spatial point processes [6], have been employed to gain quick insights into the system performance [7]. The classical analysis of wireless networks using stochastic geometry assumes a spatial model for the network elements, and averages the performance indicator (mostly outage probability) over all network states [8]. The average does not represent well the reliability of each individual link, when the standard deviation (of the indicator) is comparable to the mean. Because of that, the meta distribution of the Signal-to-Interference Ratio (SIR) has been recently proposed to assess the distribution of the outage probability, conditioned on the realization of the point process [9]. Thus far, the meta distribution of bipolar, cellular and heterogeneous wireless networks has been investigated [10], [11].

The spatial distribution of vehicles requires a model for the road infrastructure and another for the locations of vehicles conditionally on the roads. The Manhattan Poisson line process (with horizontal and vertical layout of streets) and the Poisson line process (for streets with random orientation) are popular in urban vehicular communication studies. For analytical tractability, they are coupled with one-dimensional (1D) Poisson Point Process (PPP) for the locations of vehicles along the streets. The resulting point process is commonly referred to as a Cox process in the plane. The study in [12] shows that the distribution of interference level is discontinuous at the intersections, the study in [13] brings up the trade-off between the intensities of streets and vehicles in the coverage probability (or probability of successful reception) of the typical receiver, and the study in [14] enhances the model of [13] assuming both vehicular and macro-base stations. Simpler models for the road network, e.g., two orthogonal streets in [15] and a grid of roads in [16], highlight the fact that the coverage probability of the typical receiver becomes lower near intersections, because there, the generated interference from both horizontal and vertical streets is significant.

A 1D setup should suffice for the modeling of a motorway, and it allows incorporating very realistic deployment models into connectivity studies without interference [17]. If the fading is also neglected, more network properties can be analytically evaluated, e.g., expected number of connected clusters [18]. In this paper, we are interested in V2V communication under the impact of interference and fading. In [19], a modified Matèrn hardcore type-II process is considered for the intensity of concurrent interferers per lane, and the average multi-hop packet transmission time is calculated. In [20], the 1D Matèrn type-II process is enhanced with discrete marks modeling non-saturated data traffic, and the transmission success probability is evaluated. In [21], it is shown that with low transmission probability, the outage due to 1D Bernoulli lattice converges to that due to a PPP of equal intensity.

While the studies [19]–[21] are pertinent to motorways and incorporate higher layer features (multi-hop transmission, queueing and application to automotive radars respectively),

K. Koufos and C.P. Dettmann are with the School of Mathematics, University of Bristol, BS8 1TW, Bristol, UK. {K.Koufos, Carl.Dettmann}@bristol.ac.uk

This work was supported by the EPSRC grant number EP/N002458/1 for the project Spatially Embedded Networks. All underlying data are provided in full within this paper.

they calculate the average of the performance indicator. To the best of our knowledge, the meta distribution of the SIR in VANETs has so far been studied only in [22]. Assuming a regular grid of roads and 1D PPPs for the vehicles, this (simulation-based) study indicates that the meta distribution is bimodal. Intuitively, the V2V communication in line-of-sight experiences much higher reliability than that over an intersection, making the performance of a randomly selected link either extremely reliable or totally unreliable.

Unlike the urban scenario in [22], we would like to shed some light on the meta distribution of the SIR along motorways. Naturally, the drivers maintain large safety distances in motorways, and the PPP may not model accurately the locations of vehicles [23]. In order to maintain some degree of analytical tractability while introducing more realistic deployment, we have adopted the shifted-exponential distribution for the inter-vehicle distance in [23]–[25]. This distribution has roots in transportation research [26], and it has also been used to model accidents for vehicles on the same lane [27]. More complex headway models like the log-normal distribution for multi-lane traffic in [28] are difficult to analyze. The Probability Generating Functional (PGFL) of shifted-exponential (or hardcore) point process required to calculate the moments of the meta distribution is unknown. In order to approximate the outage probability, we calculated the moments of interference under Palm (and reduced Palm) measure with respect to (w.r.t.) the shift (or hardcore distance) in [23]–[25]. Then, we selected suitable distributions for the interference level. While this approach gave good predictions for the outage probability due to the hardcore process, it is not straightforward to extend it to calculate meta distributions.

Instead of pursuing interference modeling, we will deal directly with the PGFL of the hardcore point process. Unfortunately, the bounds using first-order factorial moment expansion for Gibbs processes with conditional Papangelou intensity, see [29, Thereom 1], are not tight in the upper tail of the SIR Cumulative Distribution Function (CDF). In order to approximate the PGFL, we will split the contributions into near- and far-field. For the far-field, we model the interferers with a PPP. For the near-field, we discretize the lane into intervals equal to the hardcore distance, and we allow at most one vehicle per interval. Let us call this model, *the discretization model*. The main contributions of this paper are:

- Using the discretization model, we devise accurate approximations for the conditional PGFL and the meta distribution of the SIR due to the hardcore point process. Furthermore, we illustrate that the hardcore process (and subsequently the discretization model) approximate well the meta distribution generated from synthetic motorway traces [4], [5], while the conventional PPP fails.
- We show that introducing hardcore distance, while keeping the intensity of vehicles fixed, reduces the Coefficient-of-Variation (CoV) of the meta distribution. As a result, the conventional PPP predicts larger disparity in the performance of different links along the motorway, and it incurs large errors in the estimation of the meta distribution generated from the traces.
- We show that the CoV of the meta distribution increases for increasing SIR threshold, while all other parameters remain fixed. As a result, the calculation of the meta distribution becomes particularly meaningful in the upper tail of the SIR CDF.

In Section II, we present the system model and the discretized approximation to the hardcore process. In Section III, we calculate the PGFL for the discretization model and in Section IV its meta distribution. In Section V, we devise simple approximations for the first two moments of the meta distribution. In Section VI, we validate the models against real traces. Finally, in Section VII, we summarize the main findings and outline relevant topics for future work.

II. System model

We consider 1D point process of vehicles Φ_c, where the inter-vehicle distance follows the shifted-exponential Probability Distribution Function (PDF). The shift is denoted by $c>0$ and describes the minimum safety distance from the vehicle ahead plus the average size of a vehicle. The parameter of the exponential part is denoted by $\mu>0$ and describes the random part of inter-vehicle spacing depending on the driver's reaction time, speed, different sizes for the vehicles etc. The intensity of vehicles is $\lambda^{-1}=c+\mu^{-1}$, or $\lambda=\frac{\mu}{1+\mu c}$. We condition on the location of a transmitter at the origin. The receiver associated to it is the nearest vehicle ahead, at distance d, see Fig. 1a. We assume that only the vehicles behind the transmitter generate interference. Other vehicles may also interfere due to antenna backlobes radiation, but this would not dominate the interference level, and it is currently neglected. Hereafter, the process Φ_c denotes the points with non-negative coordinate, see Fig. 1a.

The probability to find a vehicle at $x=r>0$ follows from the Pair Correlation Function (PCF), $\rho^{(2)}(r)=\sum_{k=1}^{\infty}\rho_k^{(2)}(r)$,

$$\rho_k^{(2)}(r)=\begin{cases}\sum_{j=1}^{k}\frac{\mu^j(r-jc)^{j-1}}{\Gamma(j)e^{\mu(r-jc)}}, & r\in(kc,(k+1)c)\\ 0, & \text{otherwise},\end{cases} \tag{1}$$

$k\geq 1$ and $\Gamma(j)=(j-1)!$ [30, equation (32)].

The transmit power level is normalized to unity. The distance-based pathloss follows power-law, $r^{-\eta}$, with exponent $\eta>2$. The fading power level is independent and identically distributed (i.i.d.) over different links, following the exponential PDF with mean unity. Each interferer is active with probability ξ, independently of the activity of others.

We will now describe our novel *discretization model* which will be used to approximate the CDF and the meta distribution of the SIR due to the hardcore process. The model splits the interferers into near- and far-field depending on their locations, see Fig. 1b. The separation threshold is denoted by R. The locations of vehicles for $x>R$ are approximated by a PPP Φ_p of intensity λ, because these vehicles do not dominate the interference statistics. On the other hand, the approximating distribution for the near-field interferers considers some of the deployment contraints introduced by Φ_c: Firstly, we discretize the line segment $x\in[c,R]$ into intervals of length c, where $R=Kc, K\in\mathbb{N}_+$. Secondly, taking into account that the minimum distance separation between successive vehicles is

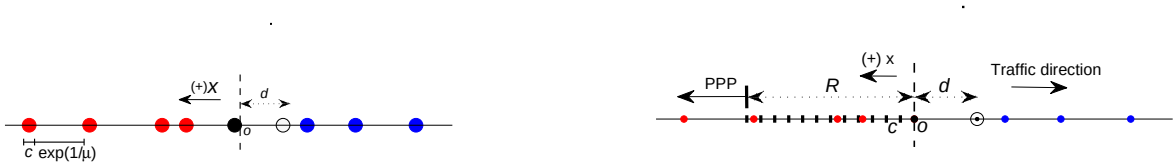

(a) Deployment model (hardcore point process)

(b) Discretization model

Fig. 1. (a) The vehicles are modeled as identical impenetrable disks of diameter c. Their antenna is placed at the right side of the disk. A transmitter (black disk) is conditioned at the origin and paired with the receiver (hollow disk) at $x=-d$. The vehicles behind the transmitter (red disks) generate interference at the receiver, while the rest (blue disks) do not. All vehicles move rightwards but the interferers are assumed in the positive half-axis to simplify the expressions. (b) The line segment $c\leq x\leq R$ is discretized with interval equal to c. The vehicles are modeled by dimensionless points located uniformly inside the discretization intervals. For $x>R$ the locations of vehicles are approximated by PPP.

c, we allow at most one vehicle inside each interval. We assume that whether an interval contains a vehicle or not is independent of other intervals. Even though this approximation may not satisfy the hardcore constraint for all vehicles, it will suffice to approximate well the PGFL of the point process Φ_c for realistic parameter settings. Furthermore, while the PDF of the location of a vehicle inside the k-th interval, $(kc,(k+1)\,c)$, is available from the PCF, we approximate it by the uniform distribution $U_k\;k\in\{1,2,\ldots,K-1\}$, to reduce the computational complexity at the cost of small accuracy loss.

Let us denote by P_k the Bernoulli-distributed Random Variable (RV) with parameter p_k, equal to the probability that the k-th interval contains a vehicle. The parameter p_k can be calculated as the integral of the PCF within $[kc,(k+1)\,c]$. For instance, for $k=1$, we have $p_1=\int_c^{2c}\mu e^{-\mu(r-c)}\mathrm{d}r=1-e^{-c\mu}$. For large k, the following simplification might be of use

$$\begin{aligned} p_k &= \int_{kc}^{(k+1)c}\rho_k^{(2)}(r)\,\mathrm{d}r \\ &\overset{(a)}{=} \sum_{j=1}^{k}\frac{\Gamma\left(j,c\mu\left(k-j\right)\right)-\Gamma\left(j,c\mu\left(k+1-j\right)\right)}{\Gamma\left(j\right)} \qquad (2)\\ &\overset{(b)}{\approx} \left(k-\frac{c\mu k}{1+c\mu}\right)-\left(k-\frac{c\mu\left(k+1\right)}{1+c\mu}\right)=\lambda c, \qquad (3)\end{aligned}$$

where $\Gamma(a,x)=\int_x^\infty\frac{t^{a-1}}{e^t}\mathrm{d}t$ is the incomplete Gamma function, (a) follows after substituting equation (1) and inter-changing the order of integration and summation, and (b) uses that for large k the function $t(x)=\frac{\Gamma(x,c\mu(k-x))}{\Gamma(x)}$ is negligible for small x and ramps up to unity after some point x_0. Therefore we may approximate the sum $\sum_{j=1}^k t(j)$ by the integral of a unit pulse between x_0 and k. Without introducing much error in the calculation of the integral, we define x_0 to be the point where $t(x_0)=\frac{1}{2}$. In order to approximate x_0, we know that $\lim_{x\to\infty}\frac{\Gamma(x,x)}{\Gamma(x)}=\frac{1}{2}$ [31]. We use this property and solve for $x_0=c\mu\left(k-x_0\right)$ or $x_0=\frac{c\mu k}{1+c\mu}$ in the first term and $x_0=\frac{c\mu(k+1)}{1+c\mu}$ in the second, and the result follows.

III. Approximating the conditional PGFL of Φ_c

Under i.i.d. Rayleigh fading, the outage probability, $\mathrm{P_{out}}(\theta)=\mathbb{P}\left(\mathrm{SIR}\leq\theta\right)$ is, see also [8, Theorem 1],

$$\mathrm{P_{out}}(\theta)=1-\mathbb{E}\Big\{\prod_{x_k\in\Phi_c\setminus\{o\}}\frac{1}{1+\xi_k s(\theta)\left(x_k+d\right)^{-\eta}}\Big\},$$

where $s\equiv s(\theta)=\theta d^\eta$, and the RVs ξ_k describe the activity of the k-th vehicle with probability ξ.
The RVs ξ_k are i.i.d. Bernoulli, and thus

$$\mathrm{P_{out}}(\theta)=1-\mathbb{E}\Big\{\prod_{x_k\in\Phi_c\setminus\{o\}}\Big(1-\xi+\xi\Big(1+s\left(x_k+d\right)^{-\eta}\Big)^{-1}\Big)\Big\}. \qquad (4)$$

The expectation in (4) should be taken over the locations of interferers and transmitter. The product is a RV describing the probability of successful reception conditioned on the locations. Its distribution is essentially the meta distribution of the SIR, as we will discuss in the next section.

After splitting the contributions to the PGFL into near- and far-field terms, and using the discretization model, we have

$$\mathrm{P_{out}}(\theta)\approx 1-\mathbb{E}\{\textstyle\prod_{x_k\in U_k}G_n(x_k)\}\mathbb{E}\Big\{\prod_{x_k\in\Phi_p}G_f(x_k)\Big\}, \qquad (5)$$

where $G_n(x_k)=1-\xi p_k+\xi p_k(1+s(x_k+d)^{-\eta})^{-1}$ for the near-field and $G_f(x_k)=1-\xi+\xi(1+s(x_k+d)^{-\eta})^{-1}$ for the far-field. For the near-field we have scaled the activity ξ with the probability the k-th interval contains a vehicle. This is valid because the RVs P_k are independent of each other and of ξ_k.

The expectation over the far-field is straightforward to compute from the PGFL of PPP within (R,∞).

$$\mathbb{E}\left\{\textstyle\prod_{x_k\in\Phi_p}G_f(x_k)\right\}=\exp\left(-\lambda\xi\int_{R+d}^\infty\frac{s}{s+x^\eta}\mathrm{d}x\right), \qquad (6)$$

where the integral can be expressed in terms of the hypergeometric ${}_2F_1$ function [32, p. 556].

The expectation for the near-field, $J_n=\mathbb{E}\{\prod_{x_k\in U_k}G_n(x_k)\}$ requires to average over a uniform distribution for the location of a vehicle inside each interval. After bringing the expectation operator inside the product we have

$$\begin{aligned} J_n &= \prod_{k=1}^{K-1}\frac{1}{c}\int_0^c\left(1-\xi p_k+\frac{\xi p_k}{1+s\left(x+a_k\right)^{-\eta}}\right)\mathrm{d}x \qquad (7)\\ &= \prod_{k=1}^{K-1}\left(1-\xi p_k+\frac{\xi p_k}{cs\left(\eta+1\right)}\left(f(a_{k+1})-f(a_k)\right)\right), \qquad (8)\end{aligned}$$

where $a_k=d+ck$, $f(a_k)=a_k^{\eta+1}{}_2F_1\left(1,\frac{\eta+1}{\eta},\frac{\eta+2}{\eta};\frac{a_k^\eta}{-s}\right)$ and p_k is given in (2).

After substituting (6) and (8) into (5), and average over the link distance d, we get an approximation for the outage probability due to the hardcore process Φ_c. We will compare the discretization model with a few other models. The first one

uses a PPP with intensity λ in (c,∞) for the interferers and a shifted-exponential PDF for the link distance. Hereafter, we will refer to it as model M1. The outage probability is

$$\mathrm{P}_{\mathrm{out}}^{\mathrm{M1}}(\theta)=1-\int_c^{\infty}\exp\left(-\lambda\xi\int_{c+r}^{\infty}\frac{s\,\mathrm{d}x}{s+x^{\eta}}\right)\mu e^{-\mu(r-c)}\mathrm{d}r. \quad (9)$$

The second model, model M2, assumes exponential PDF for the inter-vehicle distances. This is the model used in the literature for linear VANETs. The outage probability is

$$\begin{aligned}\mathrm{P}_{\mathrm{out}}^{\mathrm{M2}}(\theta) &=1-\int_0^{\infty}e^{-\lambda\xi\int_r^{\infty}\frac{\theta r^{\eta}x^{-\eta}\mathrm{d}x}{1+\theta r^{\eta}x^{-\eta}}}\lambda e^{-\lambda r}\mathrm{d}r\\ &=\frac{b(\theta)}{b(\theta)+1},\ b(\theta)=\frac{{}_2F_1\left(1,1-\frac{1}{\eta},2-\frac{1}{\eta},-\theta\right)}{(\xi\theta)^{-1}(\eta-1)}.\end{aligned} \quad (10)$$

Equation (10) is independent of the intensity. This agrees with the outage probability in the downlink of PPP interference-limited cellular networks with nearest base station association [8, Eq. (14)]. The third model M3 uses a non-homogeneous PPP with intensity $\rho^{(2)}(x)\,, x\geq 0$ and a shifted-exponential PDF for the link distance. The outage probability follows from the PGFL of PPP.

$$\begin{aligned}&\mathrm{P}_{\mathrm{out}}^{\mathrm{M3}}(\theta)\\ &=\ 1-\int_c^{\infty}\exp\left(-\int_r^{\infty}\frac{\xi s\rho^{(2)}(x-d)\,\mathrm{d}x}{s+x^{\eta}}\right)\mu e^{-\mu(r-c)}\mathrm{d}r.\end{aligned} \quad (11)$$

In order to calculate (11), we use the exact value of the PCF for distance separation up to $4c$, and the approximation $\rho^{(2)}(x)\approx\lambda$ for $(x-d)>4c$. This approximation is valid for $\lambda c\leq\frac{1}{2}$, because the correlation starts to vanish beyond that distance, see [24, Fig. 3]. Also, $\lambda c\leq\frac{1}{2}$ is reasonable for motorways [23, Fig. 8 and Fig. 9]. Finally, another approximation, model M4, yielding a closed-form expression uses a PPP of intensity λ in $(0,\infty)$ for the interferers and a shifted-exponential PDF for the link.

$$\mathrm{P}_{\mathrm{out}}^{\mathrm{M4}}(\theta)\ =1-\frac{e^{-\tilde{b}(\theta)\mu c}}{\tilde{b}(\theta)+1},\ \tilde{b}(\theta)=\frac{{}_2F_1\left(1,1-\frac{1}{\eta},2-\frac{1}{\eta},-\theta\right)}{(\xi\theta)^{-1}(1+\mu c)(\eta-1)}. \quad (12)$$

The discretization model is a tight approximation to the simulations due to the hardcore process Φ_c, see Fig. 2. The approximations in (9) and (11) perform slightly worse. The accuracy of (12) is poor, unless the transmission probability is low. This corroborates the fact that the PPP is inadequate to model interference in motorway VANETs, even if the distance distribution of the transmitter-receiver link is tuned to avoid small headways. Finally, the model M2 in (10) predicts low outage for high θ, because it allows unrealistically high link gains with high probability for the useful link.

In order to set the separation threshold R, we constrain the mean interference beyond R, $\mathbb{E}^{!o}\{\mathcal{I}\}_{x>R}$, to be less than $q\%$ of the total mean interference $\mathbb{E}^{!o}\{\mathcal{I}\}$. For $q\ll 1$, R is expected to be large, and the mean $\mathbb{E}^{!o}\{\mathcal{I}\}_{x>R}$ can be well-approximated using a PPP of intensity λ. After averaging the term $\frac{\lambda\xi}{\eta-1}(d+R)^{1-\eta}$ over the link distance d we get

$$\begin{aligned}\mathbb{E}^{!o}\{\mathcal{I}\}_{x>R}&\approx\frac{\lambda\xi}{\eta-1}\int_c^{\infty}(r+R)^{1-\eta}\,\mu e^{-\mu(r-c)}\mathrm{d}r\\ &=\frac{\lambda\xi\mu^{\eta-1}}{\eta-1}e^{\mu(c+R)}\,\Gamma(2-\eta,\mu\,(c+R))\,.\end{aligned}$$

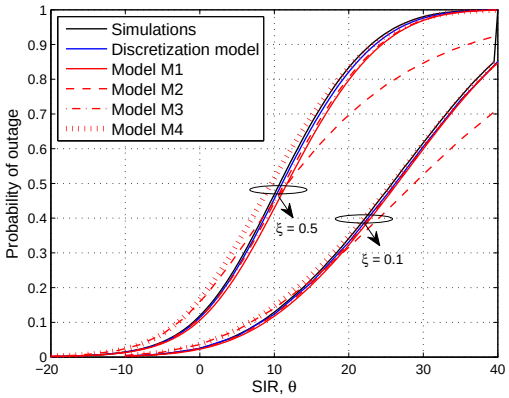

Fig. 2. Simulated probability of outage due to a hardcore point process Φ_c with $\lambda=0.025\mathrm{m}^{-1}, c=16$ m and approximations. Pathloss exponent $\eta=3$, 10^6 simulation runs. In the discretization model, $R_{min}\approx 500$ m for $q=2\%$, see (15). We set $R=512$ m, or $K=32$ units. In each simulation run: (i) We generate samples from the shifted-exponential distribution to cover a linear segment of 25 km behind the transmitter. (ii) We generate the transmitter-receiver link distance d according to the same distribution, and (iii) we generate exponentially-distributed fading and Bernoulli-distributed activity samples for all vehicles. The transmitter is assumed to be always active.

The calculation of $\mathbb{E}^{!o}\{\mathcal{I}\}$ involves the PCF in (1) which has a complicated form. Due to the fact that $\rho^{(2)}(x)\geq\mu e^{-\mu c}$ for $x\geq c$ [1], the mean interference can be bounded as

$$\begin{aligned}\mathbb{E}^{!o}\{\mathcal{I}\}&=\xi\int_c^{\infty}\int_c^{\infty}(r+x)^{-\eta}\rho^{(2)}(x)\,\mu e^{-\mu(r-c)}\mathrm{d}x\mathrm{d}r\\ &\geq\xi\int_c^{\infty}\frac{\mu e^{-\mu c}\,(r+c)^{1-\eta}}{\eta-1}\mu e^{-\mu(r-c)}\mathrm{d}r\\ &=\frac{\xi\mu^{\eta}}{\eta-1}e^{\mu c}\,\Gamma(2-\eta,2\mu c)\,.\end{aligned} \quad (13)$$

We would like to find the minimum R, denoted by R^*, satisfying $\mathbb{E}^{!o}\{\mathcal{I}\}_{x>R}\leq q\mathbb{E}^{!o}\{\mathcal{I}\}$. Since $\mathbb{E}^{!o}\{\mathcal{I}\}_{x>R}$ decreases in R, we may use the bound in (13) instead of $\mathbb{E}^{!o}\{\mathcal{I}\}$. After cancelling out common terms, we end up with

$$\min_{R>R^*}\left\{e^{\mu(c+R)}\Gamma(2-\eta,\mu\,(c+R))\leq\frac{q}{1-\lambda c}\Gamma(2-\eta,2\mu c)\right\}. \quad (14)$$

The above inequality cannot be solved in closed-form w.r.t. R. Due to the fact that R is expected to be much larger than μ^{-1}, we expand the Gamma function of the left-hand side for large $\mu R\gg 1$ obtaining: $e^{\mu(c+R)}\,\Gamma(2-\eta,\mu\,(c+R))\leq(\mu R)^{1-\eta}$. After substituting this in the left-hand side of (14), we get a bound R_{min} on the threshold, $R\geq R_{min}\geq R^*$, satisfying the constraint $\mathbb{E}^{!o}\{\mathcal{I}\}_{x>R}\leq q\mathbb{E}^{!o}\{\mathcal{I}\}$, where

$$R_{min}=\frac{1}{\mu}\left(\frac{q}{1-\lambda c}\,\Gamma(2-\eta,2\mu c)\right)^{\frac{1}{1-\eta}}. \quad (15)$$

Let us assume that we increase the intensity of the hardcore process and at the same time we impose stronger thinning, keeping constant the intensity of retained transmitters $\lambda\xi$. Under this transformation, the hardcore process converges in

[1]The minimum value of $\rho^{(2)}(x)$ for $x\geq c$ occurs at $x=2c$, see equation (1) and [24, Fig. 3] for an illustration. This bound on the PCF and thus on the mean interference is not tight for very regular point processes, e.g., $\lambda c>\frac{1}{2}$.

distribution to a PPP [10]. Simply thinning the process maintains some degree of correlation. Nevertheless, it is natural to assume that the strongly thinned process generates interference statistics similar to those of the thinned PPP. In other words, a PPP with intensity λ in (c,∞) predicts more accurately the interference field due to the process Φ_c of equal intensity for smaller ξ [21], e.g., compare the accuracy of model M1 for $\xi=0.1$ and $\xi=0.5$ in Fig. 2. Next, we show that the discretization model is consistent with this property.

Lemma 1. *For low activity ξ such that $\lambda\xi\left(R-c\right)\ll 1$ and $\lambda c\ll 1$, the outage probability due to the discretization model converges to that of a PPP given in* (9) *for all thresholds θ.*

Proof. For small ξ, equation (7) can be approximated as

$$\begin{aligned} J_n &= \prod_{k=1}^{K-1}\left(1-\frac{p_k}{c}\int_0^c \frac{\xi s\,\mathrm{d}x}{s+(x+a_k)^{\eta}}\right) \overset{(a)}{\approx} \prod_{k=1}^{K-1}\left(1-\int_0^c \frac{\lambda\xi s\,\mathrm{d}x}{s+(x+a_k)^{\eta}}\right) \\ &\overset{(b)}{\gtrapprox} 1-\sum_{k=1}^{K-1}\int_0^c \frac{\lambda\xi s\,\mathrm{d}x}{s+(x+a_k)^{\eta}} \overset{(c)}{\approx} \exp\left(-\sum_{k=1}^{K-1}\int_0^c \frac{\lambda\xi s\,\mathrm{d}x}{s+(x+a_k)^{\eta}}\right) \\ &\overset{(d)}{=} \exp\left(-\lambda\xi\int_{c+d}^{R+d}\frac{s\,\mathrm{d}x}{s+x^{\eta}}\right). \end{aligned}$$

The approximation in (a) follows from $p_k\approx\lambda c\,\forall k$. This is valid for large k, see (3), and it can also be valid for small k under the condition $\lambda c\ll 1$. For instance, $p_1=1-e^{-\frac{\lambda c}{1-\lambda c}}=\lambda c+o\left(\lambda^2c^2\right)$. The inequality in (b) is the Weierstrass product inequality $\prod_i(1-y_i)\geq 1-\sum_i y_i$, $y_i\in[0,1]$, and (c) follows from the expansion $e^{-x}\approx 1-x$, $x\to 0$. These approximations hold for $\sum_{k=1}^{K-1}\int_0^c\frac{\lambda\xi s\,\mathrm{d}x}{s+(x+a_k)^{\eta}}\leq\lambda\xi\left(K-1\right)c=\lambda\xi\left(R-c\right)\ll 1$. We get (d), which is the expression for the PGFL of a PPP in (c,R), after adding up the $(K-1)$ integral terms. After multiplying the above simplification for J_n with the far-field term in (6), we end up with the desired result. □

IV. The Meta Distribution of the SIR for Φ_c

The meta distribution of the SIR is the PDF of the probability of successful reception, $\mathrm{P}_s(\theta)$, conditioned on the spatial realization, i.e., fixed but unknown locations for the vehicles. $\mathrm{P}_s(\theta)=\mathbb{P}(\mathrm{SIR}>\theta|\Phi_c)$. The conditional probability is computed over fast fading and ALOHA, see (4).

$$\mathrm{P}_s(\theta)=\prod\nolimits_{x_k\in\Phi_c\setminus\{o\}}\left(1-\xi+\xi\left(1+s\left(x_k+d\right)^{-\eta}\right)^{-1}\right). \quad (16)$$

Due to the ergodicity of the point process Φ_c, the PDF of the RV $\mathrm{P}_s(\theta)$ is equivalent to the spatial distribution of the probability of successful reception given a realization of the point process. The complementary CDF $\mathbb{P}(\mathrm{P}_s(\theta)>u)$, $u\in[0,1]$, indicates in each realization of Φ_c, the fraction of scheduled links that experience an SIR higher than θ with probability at least u. The calculation of the PDF is not easy, but for the moments we may follow [10, Appendix]. The b-th moment, $M_b(\theta)\equiv M_b$, is computed by raising (16) to the b-th power and taking its expectation over x_k and d

$$M_b=\mathbb{E}\Big\{\prod\nolimits_{x_k\in\Phi_c\setminus\{o\}}\left(1-\xi+\xi\left(1+s\left(x_k+d\right)^{-\eta}\right)^{-1}\right)^b\Big\}.$$

Using the discretization model, the contribution to the moment M_b from the near-field can be written as

$$\begin{aligned} M_{b,n}&=\mathbb{E}\Big\{\prod\nolimits_{x_k\in U_k}\left(\frac{1}{1+s\xi_kP_k\left(x_k+d\right)^{-\eta}}\right)^b\Big\} \\ &=\mathbb{E}\Big\{\prod\nolimits_{x_k\in U_k}\left(1-\xi+\frac{\xi}{1+sP_k\left(x_k+d\right)^{-\eta}}\right)^b\Big\}. \end{aligned}$$

Taking the average w.r.t. the Bernoulli RVs P_k yields

$$M_{b,n}=\mathbb{E}\Big\{\prod_{x_k\in U_k}\left(1-p_k+p_k\left(1-\xi+\frac{\xi}{1+s\left(x_k+d\right)^{-\eta}}\right)^b\right)\Big\}. \quad (17)$$

Note that $M_{1,n}=J_n$, see (7). Next, we generalize Lemma 1 for $b>1$.

Lemma 2. *For low activity ξ such that $\lambda\xi b\left(R-c\right)\ll 1$ and $\lambda c\ll 1$, $M_{b,n}\approx\exp\left(-\lambda\xi\int_{c+d}^{R+d}1-\left(1-\frac{\xi s}{s+x^{\eta}}\right)^b\mathrm{d}x\right)\,\forall\theta$.*

Proof. Firstly, we take the expectation over x_k for each term of the product in (17) obtaining

$$M_{b,n}=\prod_{k=1}^{K-1}\left(1-p_k\left(1-\frac{1}{c}\int_0^c\left(1-\frac{\xi s}{s+(x+a_k)^{\eta}}\right)^b\mathrm{d}x\right)\right). \quad (18)$$

Secondly, we follow exactly the same steps as in the proof of Lemma 1. After substituting $p_k\approx\lambda c\,\forall k$ in $M_{b,n}$, the sufficient condition for the lemma to hold is

$$\begin{aligned} &\lambda c\sum\nolimits_{k=1}^{K-1}\left(1-\frac{1}{c}\int_0^c\left(1-\frac{\xi s}{s+(x+a_k)^{\eta}}\right)^b\mathrm{d}x\right) \overset{(a)}{\leq} \\ &\lambda c\sum\nolimits_{k=1}^{K-1}\left(1-\left(1-\xi\right)^b\right) \overset{(b)}{\approx} \lambda c\left(K-1\right)\xi b = \\ &\lambda\xi b\left(R-c\right)\ll 1, \end{aligned}$$

where (a) holds $\forall s$, and (b) is true for $\xi b\ll 1$ which is met under the condition $\lambda\xi b\left(R-c\right)\ll 1$ for $\lambda\left(R-c\right)\geq 1$, i.e., more than a single vehicle (on average) in the near-field. □

The numerical calculation of (18) can be simplified using binomial expansion in the integrand yielding

$$M_{b,n}=\prod_{k=1}^{K-1}\left(1-p_k+p_k\sum_{j=0}^{b}\binom{b}{j}\frac{h(a_{k+1},j)-h(a_k,j)}{(-\xi)^{-j}}\right), \quad (19)$$

where $h(a_k,j)=\frac{a_k}{c}{}_2F_1\left(j,\frac{1}{\eta},\frac{\eta+1}{\eta};\frac{a_k^{\eta}}{-s}\right)$.

The contribution $M_{b,f}=\mathbb{E}\Big\{\prod_{x_k\in\Phi_p}G_f(x_k)^b\Big\}$, uses the PGFL of PPP, see [33, App. A].

$$\begin{aligned} M_{b,f}&=\exp\left(-\lambda\int_{R+d}^{\infty}1-\left(1-\frac{\xi s}{s+x^{\eta}}\right)^b\mathrm{d}x\right) \\ &=\exp\left(\lambda\sum_{j=1}^{b}\binom{b}{j}\left(-\xi s\right)^j\underbrace{\int_{R+d}^{\infty}\frac{\mathrm{d}x}{(s+x^{\eta})^j}}_{F_j}\right), \end{aligned} \quad (20)$$

where $F_j=\frac{(R+d)^{1-j\eta}}{(j\eta-1)}{}_2F_1\left(j-\frac{1}{\eta},j,j-\frac{1}{\eta}+1;-s\left(R+d\right)^{-\eta}\right)$.

The moment M_b is calculated by multiplying (19) with (20) before averaging over the shifted-exponential distribution for the link distance. The integration becomes computationally demanding for high b hence, we will calculate only the first two moments, and match them to a Beta PDF $g(z)=$

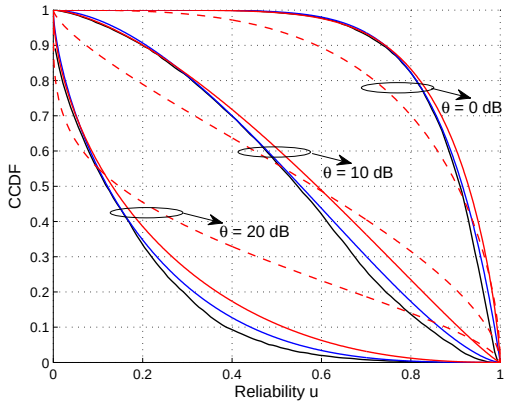

Fig. 3. The simulated meta distribution of the SIR for a hardcore process with intensity $\lambda = 0.025\text{m}^{-1}$, $c = 16\text{m}$ and $\xi = 0.5$ (black lines), and the Beta approximations using the discretization model (blue lines) and the models M1 (solid red lines) and M2 (dashed red lines). The simulations are generated using 10^4 spatial configurations with 10^4 realizations of fading and activity per configuration. See the caption of Fig. 2 for other parameter settings.

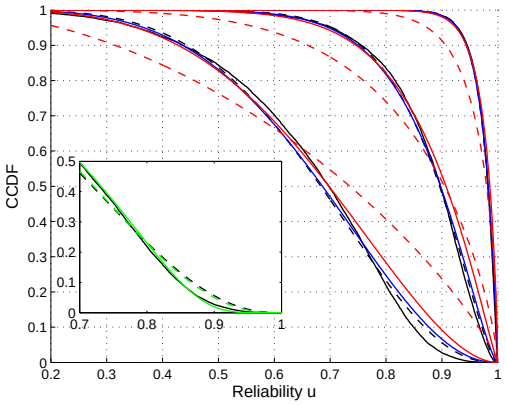

Fig. 4. The meta distribution of the SIR for a hardcore process with activity $\xi = 0.1$. See the caption of Fig. 3 for other parameter settings and explanation of line styles. The black dashed lines correspond to a Beta approximation using the simulated mean and variance due to the hardcore process. This is to illustrate that for low activity and large thresholds θ, the Beta approximation may not be very accurate at the tail. In the inset, we illustrate that for threshold 20 dB, a generalized Beta PDF with two parameters (green dashed line), $g(z) = \alpha\beta z^{\alpha-1}\left(1-z^{\alpha}\right)^{\beta-1}$, gives a marginal improvement, and with three parameters (green solid line), $g(z) = \frac{\alpha}{\mathrm{B}(\epsilon,\beta)} z^{\alpha\epsilon-1}\left(1-z^{\alpha}\right)^{\beta-1}$, matching also the skewness, gives almost a perfect fit. The penalty paid in both cases is the numerical iterative calculation of their parameters.

$\frac{1}{\mathrm{B}(\alpha,\beta)} z^{\alpha-1}\left(1-z\right)^{\beta-1}$, $\alpha,\beta>0$, where $\mathrm{B}(\alpha,\beta) = \frac{\Gamma(\alpha)\Gamma(\beta)}{\Gamma(\alpha+\beta)}$. The Beta approximation has been widely adopted for meta distributions [10], [11]. Its parameters are $\alpha = \frac{m_1(m_1(1-m_1)-m_2)}{m_2}$ and $\beta = m_1 - 1 + \frac{m_1(1-m_1)^2}{m_2}$, where $m_1 = M_{1,n}M_{1,f}$ and $m_2 = M_{2,n}M_{2,f} - m_1^2$. [10, Sec. II-F].

We will also approximate the meta distribution due to the models M1 and M2. In Fig. 2, we saw that the model M3 involves much more complicated integration than M1 without obvious benefits. The model M4 improves the prediction as compared to M2 but not as much as M1. For the model M1 the moments M_b are calculated after substituting $R = c$ in (20) and averaging over $\mu e^{-\mu(r-c)}, r > c$. For the model M2 the moments are computed after substituting $R = 0$ in (20) and averaging over $\lambda e^{-\lambda r}, r > 0$. For all models we will apply the method of moments with Beta approximation.

The simulated meta distribution due to the hardcore process and the various approximations are depicted in Fig. 3. The first point to remark is that M2 can be very unreliable, especially for large thresholds, – it significantly overestimates both moments, see also Fig. 2. Correcting M2 using M1 already brings a major improvement, which can be enhanced further using the discretization model. Reading from the figure, M2 predicts that 70% of scheduled links achieve a SIR of 0 dB with probability at least 0.8 while, the other models predict very accurately the correct fraction 83% of links. Another remark from Fig. 3 is that for low thresholds θ, the CoV of the meta distribution decreases, which means that most of the scheduled links will experience about the same reliability. The meta distribution for activity $\xi = 0.1$ is depicted in Fig. 4.

V. Properties of the meta distribution

In this section we study the behaviour of the moments M_1, M_2 and the CoV of the meta distribution w.r.t. the activity and the SIR threshold. In addition, we devise low-complexity approximations for these terms, which turn out to be much more accurate than the predictions using the model M2.

Lemma 3. *For $\lambda c \ll 1$, the CoV of the meta distribution for the discretization model as $\xi \to 0$, $\theta \to \infty$ such that $\xi\theta^{\frac{1}{\eta}} = T$, where $T > 0$ is constant, converges to $\frac{\nu}{\sqrt{\mu(\mu+2\nu)}}$, where $\nu = \lambda T \frac{\eta^2+1}{\eta^2-1}$.*

Proof. For $\xi \to 0$, the condition $\lambda\xi b\left(R-c\right) \ll 1, b \in \{1,2\}$ is satisfied for realistic λ, c, R. In addition $\lambda c \ll 1$ hence, the assumptions in Lemma 2 hold. Therefore the moments M_1, M_2 due to the discretization model can be approximated using the model M1. The first moment due to M1, see (9), is

$$M_1 = \int_c^{\infty} e^{-\lambda\xi \int_{c+r}^{\infty} \frac{\theta r^{\eta} \mathrm{d}x}{\theta r^{\eta} + x^{\eta}}} \mu e^{-\mu(r-c)} \mathrm{d}r. \tag{21}$$

For large θ, the integral w.r.t. x in (21) accepts the following approximation.

$$\int_{c+r}^{\infty} \frac{\theta r^{\eta} \mathrm{d}x}{\theta r^{\eta} + x^{\eta}} \overset{(a)}{\approx} \int_{c+r}^{r\theta^{\frac{1}{\eta}}} \left(1 - \frac{x^{\eta}}{\theta r^{\eta}}\right) \mathrm{d}x + \int_{r\theta^{\frac{1}{\eta}}}^{\infty} \theta r^{\eta} x^{-\eta} \mathrm{d}x \quad = \quad \frac{\eta^2+1}{\eta^2-1} r\,\theta^{\frac{1}{\eta}} - (c+r) + \frac{(c+r)^{1+\eta} r^{-\eta}}{(\eta+1)\theta} \approx \frac{\eta^2+1}{\eta^2-1} r\,\theta^{\frac{1}{\eta}} - (c+r),$$

where (a) follows from expanding the fraction (up to first-order) for small $x < \theta^{1/\eta} r$ in the first term, and large $x > \theta^{1/\eta} r$ in the second term.

After substituting the above approximation in (21), and carrying out the integration w.r.t. r, we end up with

$$M_1 \approx e^{\lambda c \xi} \frac{\mu e^{-\nu_1 c}}{\mu + \nu_1},\ \nu_1 = \lambda\xi\left(\frac{\eta^2+1}{\eta^2-1}\theta^{\frac{1}{\eta}} - 1\right). \tag{22}$$

Similarly, for the second moment we get

$$\begin{aligned} M_2 &\approx e^{2\lambda c\xi - \lambda\xi^2 c} \frac{\mu e^{-\nu_2 c}}{\mu + \nu_2}, \\ \nu_2 &= 2\lambda\xi\left(\tfrac{\eta^2+1}{\eta^2-1}\theta^{\frac{1}{\eta}} - 1\right) - \lambda\xi^2\left(\tfrac{4\eta^3+3\eta+1}{(\eta+1)(4\eta^2-1)}\theta^{\frac{1}{\eta}} - 1\right). \end{aligned} \tag{23}$$

After substituting $\theta^{\frac{1}{\eta}} = T\xi^{-1}$ in ν_1, ν_2 and taking the limit of M_1, M_2 for $\xi \to 0$, we get

$$\lim_{\xi\to 0} M_1 = \frac{\mu e^{-\nu c}}{\mu + \nu},\ \lim_{\xi\to 0} M_2 = \frac{\mu e^{-2\nu c}}{\mu + 2\nu}. \tag{24}$$

TABLE I
THE DISCRETIZATION MODEL, THE MODEL M1, AND THE APPROXIMATIONS (22), (23) PREDICT WELL THE MOMENTS M_1, M_2 AND THE COV OF THE META DISTRIBUTION DUE TO THE SIMULATED HARDCORE PROCESS. THE MODEL M2 FAILS IN THE ESTIMATION OF COV. EACH TERM IS ROUNDED AT THE FIFTH DECIMAL DIGIT. $\xi=10^{-2}$, $\theta=10^3$, SEE THE CAPTION OF FIG. 3 FOR OTHER PARAMETER SETTINGS.

	M_1	M_2	CoV	
Discretization model	0.89968	0.81293	0.06580	
Model M1	0.90050	0.81456	0.06729	
Lemma 3, (22) and (23)	0.89698	0.80846	0.06954	
Model M2	0.90015	0.81891	0.10322	
Simulations hardcore	0.89811	0.81010	0.06579	

Finally, writing the CoV as $\sqrt{\frac{M_2}{M_1^2}-1}$, and substituting the limits from (24) yields the desired result. The limits depend on ξ, θ through the product $\xi\theta^{1/\eta}$, while the approximations (22) and (23) depend also individually on ξ. □

In order to illustrate the usefulness of Lemma 3, let us assume early penetration of VANETs, with activity $\xi=10^{-2}$. Let us also consider a high-rate data communication at $\theta=30$ dB, yielding $T=0.1$ for $\eta=3$. The numerical calculation of the moments M_1, M_2 and the CoV using various models are presented in Table I. The model M1 is a good approximation to the discretization model because the activity is low. The approximations (22) and (23) follow closely the results due to M1, because the threshold θ is large. In addition, the limit ($\xi\to 0$) for the CoV in Lemma 3 works well yielding, $\frac{\nu}{\sqrt{\mu(\mu+2\nu)}} = 0.070$. Neglecting the hardcore distance, i.e., $\mu=\lambda$ and $\frac{\nu}{\sqrt{\lambda(\lambda+2\nu)}}=0.112$ incurs large error, because the link gain experiences much higher variability for $c=0$ than for $c=16$, while λ is fixed. In Fig. 5, it is illustrated that the approximations in (22) and (23) are good also for realistic activity values, e.g., up to $\xi=0.2$. For $\xi=0.5$ we obtain $\theta=1$ for $T=0.5$, and the approximations in (22), (23) break down.

The limit of the CoV in Lemma 3 increases in ν and thus in θ, while ξ is kept constant, see Fig. 6 for an illustration. This is also evident by visual inspection from Fig. 3, where the variance of the meta distribution is much less for $\theta=1$ than for $\theta=100$. The large CoVs mean that the average success probability M_1 does not represent well the performance of different links across a snapshot of the network. Furthermore, Lemma 3 indicates that for low and decreasing activity $\xi\to 0$, while keeping constant M_1 by increasing θ, the variance of the conditional success probability across the network does not become zero. This is in accordance with [10, Corollary 7] for cellular networks with random activity. In Fig. 5, for $M_1\approx 0.566$ and activity $\xi\to 0$, the standard deviation of the conditional success probability converges to 0.16. Finally, according to (24), for $\eta>2$ and $\theta\geq 1$, M_1, M_2 increase for increasing η but the CoV decreases. Intuitively, higher pathloss means that links scheduled at the same time are better isolated from each other, and the fraction of links achieving certain reliability should increase, see also Fig. 8 and Fig. 9.

Next, we present approximations for M_1, M_2 and CoV for $\theta\ll 1$. For small θ, the model M1 approximates well the discretization model even for large activity, see Fig. 2 and Fig. 3 for example illustrations.

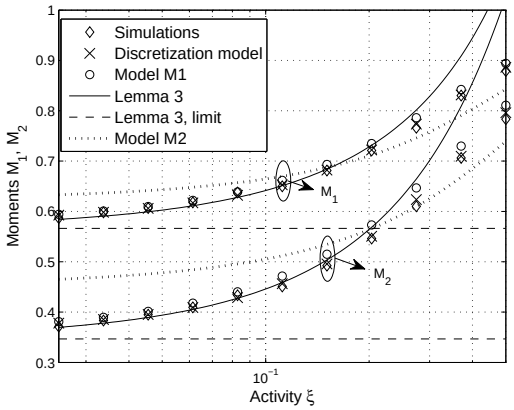

Fig. 5. The moments M_1, M_2 for pairs (ξ,θ) satisfying $T=\xi\theta^{1/\eta}=0.5$. The discretization model, the model M1 and the approximations (22) and (23) in Lemma 3 estimate accurately the moments due to the simulated hardcore process. The model M2 fails. See the caption of Fig. 3 for other parameters.

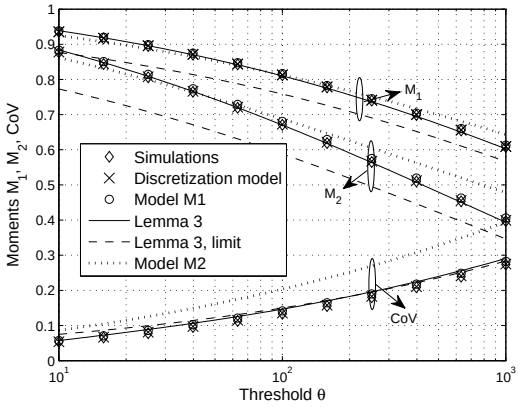

Fig. 6. The moments M_1, M_2 and the CoV for activity $\xi=0.05$ and large thresholds θ. The discretization model, the model M1 and the approximations (22), (23) give very good predictions to the simulated hardcore process, while M2 fails. The limit for the CoV in Lemma 3 increases approximately by $\theta^{1/2\eta}$ for large θ. See the caption of Fig. 3 for other parameter settings.

Lemma 4. *For $\theta\ll 1$, the CoV of the meta distribution for the discretization model is approximated by $\frac{\nu^*}{\sqrt{\mu(\mu+2\nu^*)}}$, where $\nu^*=\frac{(\eta+1)\lambda t}{2^\eta(\eta-1)}$ and $t=\xi\theta\ll 1$ is a positive constant.*

Proof. For small θ, equation (21) can be approximated as

$$M_1 \approx \int_c^\infty e^{-\lambda\xi\int_{c+r}^\infty \theta r^\eta x^{-\eta}\mathrm{d}x}\mu e^{-\mu(r-c)}\mathrm{d}r$$
$$= \int_c^\infty e^{-\frac{\lambda\xi\theta}{\eta-1}r^\eta(r+c)^{1-\eta}}\mu e^{-\mu(r-c)}\mathrm{d}r.$$

For small θ, we get $\mu > \frac{\lambda\xi\theta}{\eta-1}$, which means that the term $e^{-\mu r}$ dominates the integrand. In addition, the main contribution to the integral is given by the vicinity of c. Because of that, we can expand the term $r^\eta\,(r+c)^{1-\eta}$ around c, without introducing much error. After expanding up to the first order and carrying out the integration, we end up with

$$M_1 \approx e^{\frac{\lambda c t}{2^\eta}}\,\frac{\mu e^{-\nu^* c}}{\mu+\nu^*}. \tag{25}$$

Similarly, the approximation of M_2 for $\theta\ll 1$, keeping only

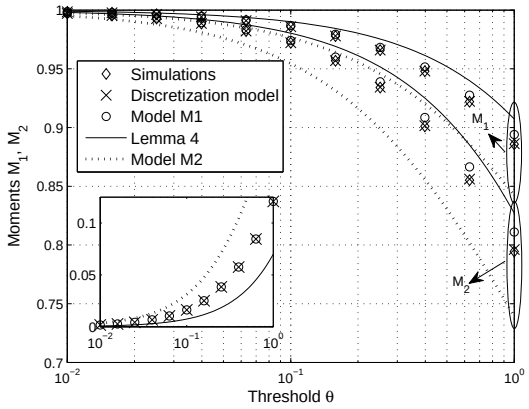

Fig. 7. The moments M_1, M_2 for activity $\xi = 0.5$ and small thresholds θ. The discretization model and the model M1 predict well the simulated moments due to the hardcore process. The approximations (25), (26) give better predictions than M2. The CoV (see the inset) is approximately proportional to θ for small θ, see Lemma 4. See the caption of Fig. 3 for other parameters.

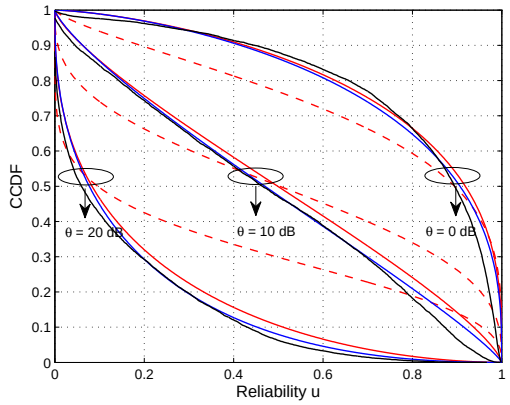

Fig. 10. Meta distributions for the 1200-th snapshot from motorway M40, May 7 2010, busy hour, left lane, considering interference from all three lanes. For lane separation 4 m and antenna beamwidth $\frac{\pi}{20}$ we have $r_0 \approx 50$ m for the middle lane and $2r_0 \approx 100$ m for the right lane. For the right lane, we assume a PPP beyond $2r_0$ for all three models with $\lambda_r \approx 0.0205\,\mathrm{m}^{-1}$. For the middle lane we assume PPP beyond r_0 for the models M1 and M2 with $\lambda_m \approx 0.0186\,\mathrm{m}^{-1}$. For the discretization model we estimate $\lambda_m \approx 0.0193\,\mathrm{m}^{-1}, c_m \approx 9.86$ m, and $K_m = 14$ for $q = 2\%$. $\eta = 4$, see the caption of Fig. 9 for other parameter settings and mapping of line styles to models.

the leading-order term w.r.t. t, is

$$M_2 \approx e^{\frac{\lambda c t}{2^{\eta-1}}} \frac{\mu e^{-2\nu^* c}}{\mu + 2\nu^*}. \tag{26}$$

The approximations (25) and (26) depend on ξ and θ only through their product. After substituting (25), (26) into $\sqrt{\frac{M_2}{M_1^2} - 1}$, the result of the lemma follows. □

The approximations (25), (26) are validated in Fig. 7. Summing up, according to Lemma 3, if we reduce the activity by 10 dB, we can increase the threshold θ by 10η dB to maintain the same probability of success M_1 for large θ and $\xi \to 0$. According to Lemma 4, for low θ, we can increase the threshold only by 10 dB. For instance, in Fig. 2, the probability of outage at -10 dB is 0.014 with activity $\xi = 0.5$. The same outage with activity $\xi = 0.1$, occurs around -3 dB confirming (25). Note also that according to (26), the two pairs $(\xi, \theta) \in \{(0.5, -10\text{dB}), (0.1, -3\text{dB})\}$ result in the same second moment M_2 too. On the other hand, the probability of outage at 10 dB is 0.45 with activity $\xi = 0.5$ in Fig. 2, while with activity $\xi = 0.1$ the same outage occurs at 24.5 dB, instead of 31 dB predicted by (24). This is because (24) is valid for $\xi \to 0$, and (22) should be used instead. Finally, the CoVs calculated in the Lemmas decrease in c, while the intensity λ is fixed. This is clear after writing the CoV as $\frac{\nu\mu^{-1}}{\sqrt{1+2\nu\mu^{-1}}}$, where $\nu\mu^{-1} \propto (1 - \lambda c)$, see Fig. 6 and the inset in Fig. 7 for the comparison between M2 and the Lemmas.

VI. Validation with real traces

Thanks to [4], [5], there are publicly available traces for three-lane unidirectional motorway traffic. In order to generate them, the studies have collected per-lane measurements every second about the number of passing vehicles and their speed, using induction loops at a measurement location outside Madrid in Spain. The measurements have been used to calibrate a simulator modeling micro-mobility features like lane-changing pattern, velocity distributions etc. The output of the simulator is the location of vehicles, i.e., lane and horizontal position over a road segment of 10 km with one second granularity. In [23] we have analyzed these traces using the J- and the Ripley's K-function [34, Ch. 2.8]. We have illustrated that the PPP cannot capture the distribution of inter-vehicle distances, because it permits unrealistically small distances with high probability. The PPP becomes more problematic for the left lane because due to the high speeds over there, the drivers maintain large safety distances. We have illustrated that the envelope of the J-function for the fitted hardcore process Φ_c can capture the J-function of the real snapshot, see [23, Sec. IV] for a detailed description of the fitting method.

In the current paper, we use the fitted parameters λ, c to assess which model (discretization, M1 and M2) can better predict the simulated outage probability and the meta distribution of snapshots. We see in Fig. 8 that for the left lane of the selected snapshot, $\lambda c \approx 0.3$, the discretization model outperforms the model M1, especially for large thresholds, while M2 incurs very large errors. Higher spatial regularity, $\lambda c \approx 0.4$ in Fig. 9, makes clear the benefit of discretization.

The extension of the discretization model to multiple lanes is straightforward by discretizing with lane-specific parameter c. Due to directionality, only vehicles behind some distance r_0 from the receiver may contribute to other-lane interference, see [23, Section VI]. The interference originated from other lanes does not require to constrain the location of any of the points of the processes. We just add a reference point (the receiver) at the origin. The separation threshold between near- and far-field interferers for other lanes is easier to calculate. Starting from $\int_R^\infty r^{-\eta} \mathrm{d}r \leq q \int_{r_0}^\infty r^{-\eta} \mathrm{d}r$, we have $R \geq (1/q)^{\frac{1}{\eta-1}} r_0$. The results are available in Fig. 10. Summing up, Fig. 8 – Fig. 10 highlight the discretization model as a reasonable choice for modeling the outage probability along motorway VANETs.

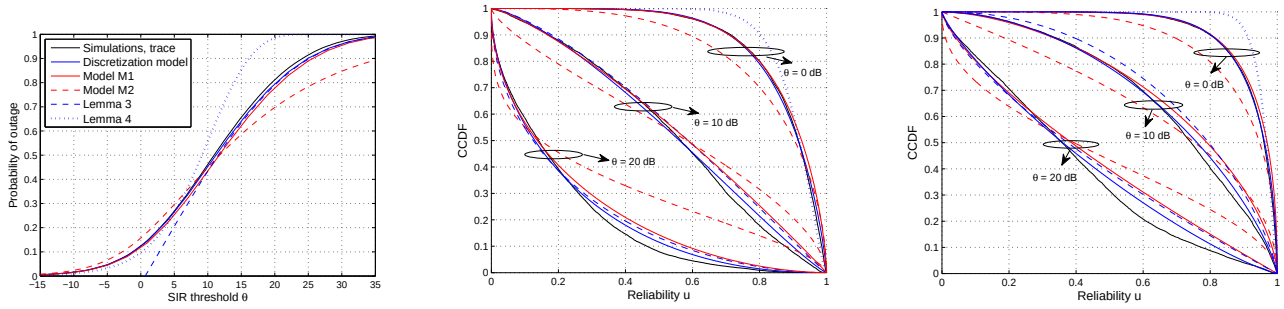

(a) Outage probability, $\eta = 3$ (b) Meta distribution, $\eta = 3$ (c) Meta distribution, $\eta = 4$

Fig. 8. (a) The simulated probability of outage using real trace and the approximations using the discretization model, and the models M1 and M2. For the discretization model and M1, the (fitted) shifted-exponential PDF has $\lambda \approx 0.0205\,\mathrm{m}^{-1}$ and $c \approx 14.82\,\mathrm{m}$, yielding $\lambda c \approx 0.3037$. For M2, the (fitted) exponential PDF has $\lambda \approx 0.0195\,\mathrm{m}^{-1}$. For $q = 2\%$, we get $R_{min} \approx 442\,\mathrm{m}$ from (15), and we calculate $K = \lceil \frac{R_{min}}{c} \rceil = 30$ and $R = Kc \approx 445\,\mathrm{m}$. 10^5 simulations. The approximation (22) in Lemma 3 for large thresholds is accurate for $\theta > 10$, and the approximation (25) in Lemma 4 for small thresholds is accurate for $\theta < 0.5$. (b)-(c) The simulated meta distribution and the approximations using the same models. 10^4 spatial configurations and 10^4 realizations of fading and activity per configuration. The approximations (22) and (23) coupled with the Beta approximation are depicted for large thresholds $\theta = 10$ and $\theta = 100$. For $\theta = 1$, we used the approximations (25) and (26), which are not accurate because Lemma 4 assumes small $\theta \ll 1$. Activity $\xi = 0.5$. We have selected the 1000-th snapshot from motorway M40, May 7 2010, busy hour [4], [5]. The empirical CDF of inter-vehicle distances, obtained from the trace, is used to simulate the locations of interferers and the useful link distance.

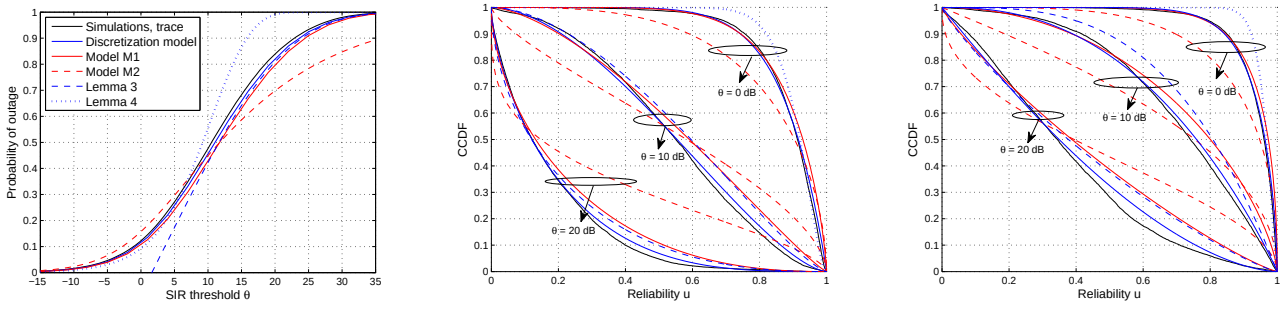

(a) Outage probability, $\eta = 3$ (b) Meta distribution, $\eta = 3$ (c) Meta distribution, $\eta = 4$

Fig. 9. Fitting the models to the simulations using the 1200-th snapshot from motorway M40, May 7 2010, busy hour [4], [5]. For the discretization model and the model M1 we use the estimates $\lambda \approx 0.0203\,\mathrm{m}^{-1}$, $c \approx 19.76\,\mathrm{m}$, resulting to $\lambda c \approx 0.4017$. For the model M2 we estimate $\lambda \approx 0.0191\,\mathrm{m}^{-1}$. See the caption of Fig. 8 for explanation of the legend and other parameter settings.

VII. Conclusions

In high-speed motorways the vehicles maintain large safety distances from the vehicle ahead. Because of that, a shifted-exponential PDF captures the distribution of headway distance along a lane much better than the PPP. In order to approximate the PGFL of the shifted-exponential (or hardcore) process, we used a shifted-exponential PDF for the link distance coupled with a guard zone (equal to the hardcore distance) behind the transmitter. This model predicts the moments of the SIR much better than the PPP. Nevertheless, for regular deployments, and/or large SIR threshold and transmission probability, it starts to lose some of its power. Because of that, we have devised a discretized deployment for the near-field. This is more tailored to the hardcore constraints, hence it approximates better the PGFL of the hardcore process. The discretization model coupled with the Beta PDF for the meta distribution can capture the statistics of the outage probability along a lane of the motorway. This has been validated against synthetic traces generated from real vehicular data, considering also interference due to multiple lanes. The discretization model would be useful for network planning, because it provides the system designer with better prediction of the distribution of outage probabilities than that obtained with a PPP.

We have shown that for increasing SIR thresholds the disparity in the success probability across different links increases. This means that the upper tail of the SIR CDF, calculated as an average over all spatial realizations, does not represent accurately the outage probability along a snapshot of the motorway. As a result, the calculation of the meta distribution becomes useful. We have also shown that the PPP predicts much higher disparity than that observed with real traces, because it allows more variability in the link distance. Another important conclusion is that the mean and the variance of the meta distribution in the low SIR depend only on the product of transmission probability and SIR threshold. Therefore lowering the activity by x dB allows increasing the operation threshold by x dB with little effect on the meta distribution. This is, however, not the case for high SIR thresholds. Regarding future work, it would be good to see the calculation of the meta distribution also for the rate statistics. In addition, it would be interesting to study

the joint distribution of the SIR over multiple slots, which is related to the design of retransmission schemes for VANETs. Some preliminary analysis about the temporal statistics of interference under the hardcore point process can already be found in [35].

ACKNOWLEDGMENT

The authors would like to thank Harpreet Dhillon for helpful discussions.

REFERENCES

[1] A. Filippi *et.al.*, "Ready to roll: Why 802.11p beats LTE and 5G for V2X", White paper, NXP Semiconductors, Cohda Wireless and Siemens, 2016.

[2] FCC Report and Order 03-324: Amendment of the Commission's rules regarding dedicated short-range communication services in the 5.850-5.925 GHz band, 2003.

[3] S. Chen *et.al.*, "Vehicle-to-everything (V2X) services supported by LTE-based systems and 5G", *IEEE Commun. Standards Mag.*, vol. 1, no. 2, pp. 70-76, Jul. 2017.

[4] M. Gramaglia *et.al.*, "Vehicular networks on two Madrid highways", *in Proc. IEEE Int. Conf. Sensing, Commun. and Networking (SECON)*, Singapore, Jun. 2014, pp. 423-431.

[5] M. Gramaglia *et.al.*, "Mobility and connectivity in highway vehicular networks: A case study in Madrid", *Elsevier Comput. Commun.*, vol. 78, pp. 28-44, 2016.

[6] D.J. Daley, and D. Vere-Jones, An introduction to the theory of point processes: Volume I: Elementary theory and methods. Springer, ISBN 0-387-95541-0, 2002.

[7] W. Lu and M.D. Renzo, "Stochastic geometry modeling of cellular networks: Analysis, simulation and experimental validation", *in Proc. 18th ACM Int. Conf. Modeling, Analysis and Simulation Wireless and Mobile Syst.*, Mexico, 2015, pp. 179-188.

[8] J.G. Andrews, F. Baccelli and R.K. Ganti, "A tractable approach to coverage and rate in cellular networks", *IEEE Trans. Commun.*, vol. 59, pp. 3122-3134, Nov. 2011.

[9] R.K. Ganti, J.G. Andrews, "Correlation of link outages in low-mobility spatial wireless networks", *44th Asilomar Conf. Signals, Syst. and Comput.*, Pacific Grove, 2010.

[10] M. Haenggi, "The meta distribution of the SIR in Poisson bipolar and cellular networks", *IEEE Trans. Wireless Commun.*, vol. 15, pp. 2577-2589, Apr. 2016.

[11] Y. Wang, M. Haenggi and Z. Tan, "The meta distribution of the SIR for cellular networks with power control", *IEEE Trans. Commun.*, vol. 66, pp. 1745-1757, Apr. 2018.

[12] F. Baccelli and X. Zhang, "A correlated shadowing model for urban wireless networks", *in Proc. IEEE Int. Conf. Comput. Commun. (INFOCOM)*, Hong Kong, 2015, pp. 801-809.

[13] V.V. Chetlur and H.S. Dhillon, "Coverage analysis of a vehicular network modeled as Cox Process driven by Poisson Line Process", *IEEE Trans. Wireless Commun.*, vol. 17, pp. 4401-4416, Jul. 2018.

[14] C.-S. Choi and F. Baccelli, "An analytical framework for coverage in cellular networks leveraging vehicles", *IEEE Trans. Commun.*, vol. 66, no. 10, pp. 4950-4964, Oct. 2018.

[15] E. Steinmetz, M. Wildemeersch, T. Quek and H. Wymeersch, "A stochastic geometry model for vehicular communication near intersections", *in Proc. IEEE Global Commun. Conf. (Globecom) Workshops*, San Diego, 2015, pp. 1-6.

[16] J.P. Jeyaraj and M. Haenggi, "Reliability analysis of V2V communications on orthogonal street systems", *in Proc. IEEE Global Commun. Conf. (Globecom) Workshops*, Singapore, Dec. 2017.

[17] C. Shao *et.al.*, "Performance analysis of connectivity probability and connectivity-aware MAC protocol design for platoon-based VANETs", *IEEE Trans. Veh. Technol.*, vol. 64, pp. 5596-5609, Dec. 2015.

[18] S. Kwon, Y. Kim and N.B. Shroff, "Analysis of connectivity and capacity in 1-D vehicle-to-vehicle networks", *IEEE Trans. Wireless Commun.*, vol. 15, pp. 8182-8194, Dec. 2016.

[19] M.J. Farooq, H. ElSawy and M.-S. Alouini, "A stochastic geometry model for multi-hop highway vehicular communication", *IEEE Trans. Wireless Commun.*, vol. 15, pp. 2276-2291, Mar. 2016.

[20] Z. Tong, H. Lu, M. Haenggi and C. Poellabauer, "A stochastic geometry approach to the modeling of DSRC for vehicular safety communication", *IEEE Trans. Intell. Transp. Syst.*, vol. 17, pp. 1448-1458, May 2016.

[21] A. Al-Hourani *et.al.*, "Stochastic geometry methods for modeling automotive radar interference", *IEEE Trans. Intell. Transp. Syst.*, vol. 19, no. 2, pp. 333-344, Feb. 2018.

[22] M. Abdulla and H. Wymeersch, "Fine-grained vs. average reliability for V2V communications around intersections", *in Proc. IEEE Global Commun. Conf. (Globecom) Workshops*, Singapore, Dec. 2017, pp. 1-5.

[23] K. Koufos and C.P. Dettmann, "Outage in motorway multi-lane VANETs with hardcore headway distance using synthetic traces", submitted for publication, available at https://arxiv.org/abs/1901.06368.

[24] K. Koufos and C.P. Dettmann, "Moments of interference in vehicular networks with hardcore headway distance", *IEEE Trans. Wireless Commun.*, vol. 17, pp. 8330-8341, Dec. 2018.

[25] K. Koufos and C.P. Dettmann, "Performance of a link in a field of vehicular interferers with hardcore headway distance", submitted for publication, available at https://arxiv.org/abs/1810.00959.

[26] R.J. Cowan, "Useful headway models", *Transportation Research*, vol. 9, no. 6, pp. 371-375, Dec. 1975.

[27] S.-L. Sou, "Modeling emergency messaging for car accident over dichotomized headway model in vehicular ad-hoc networks", *IEEE Trans. Commun.*, vol. 61, pp. 802-812, Feb. 2013.

[28] N. Nawaporn *et.al.*, "Routing in sparse vehicular ad hoc wireless networks", *J. Sel. Areas Commun.*, vol. 25, no. 8, pp. 1538-1556, Oct. 2007.

[29] K. Stucki and D. Schumacher, "Bounds for the probability generating functional of a Gibbs point process", *J. Advances Appl. Probability*, vol. 46, no. 1, pp. 21-34, Mar. 2014.

[30] Z.W. Salsburg, R.W. Zwanzig and J.G. Kirkwood, "Molecular distribution functions in a one-dimensional fluid", *J. Chemical Physics*, vol. 21, pp. 1098-1107, Jun. 1953.

[31] W. Gautschi, "The incomplete Gamma functions since Tricomi", *in Tricomi's ideas and Contemporary Appl. Math.*, pp. 203-237, 1998.

[32] M. Abramowitz and I.A. Stegun. Handbook of mathematical functions with formulas, graphs and mathematical tables. Washington, DC, USA: GPO, 1972.

[33] M. Haenggi and R. Smarandache, "Diversity polynomials for the analysis of temporal correlations in wireless networks", *IEEE Trans. Wireless Commun.*, vol. 12, pp. 5940-5951, Nov. 2013.

[34] M. Haenggi, Stochastic geometry for wireless networks. Cambridge University Press, 2013.

[35] K. Koufos and C.P. Dettmann, "Temporal correlation of interference in vehicular networks with shifted-exponential time headways", *IEEE Wireless Commun. Lett.*, vol. 8, pp. 189-192, Feb. 2019.